large Exploring the Structure of the Proton via Semi-inclusive Pion Electroproduction

N. Harrison et al[1]

(The CLAS Collaboration)

[1] *Thomas Jefferson National Accelerator Facility, Newport News, Virginia 23606*
(Dated: May 11, 2016)

We present studies of multiplicities and the $\cos\phi$, and $\cos 2\phi$ moments, in charged pion production in semi-inclusive deep inelastic scattering (SIDIS). The data set used was the E1-f run from the CEBAF Large Acceptance Spectrometer (CLAS) at Jefferson Lab which ran in 2003. The run used a 5.498 GeV longitudinally polarized electron beam and an unpolarized liquid hydrogen target. Two pion channels ($\pi+$ and $\pi-$) were studied over a broad kinematical range ($x = 0.1 - 0.6$, $Q^2 = 1.0 - 4.5$ GeV^2, $z = 0.0 - 1.0$, $P_{h\perp}^2 = 0.0 - 1.0$ GeV^2, and $-180° < \phi_h < 180°$). These measurements give insights into the transverse momentum dependence of parton distribution functions (PDFs) describing the dynamics of quarks and gluons inside of the proton.

PACS numbers:

In recent years parton distribution functions have been generalized to contain information not only on the longitudinal momentum but also on the transverse momentum distributions of partons in a fast moving hadron. Intense theoretical investigations of Transverse Momentum Dependent (TMD) distributions of partons and the first unambiguous experimental signals of TMDs indicate that QCD-dynamics inside hadrons is much richer than what can be learned from collinear parton distributions. It is expected that TMDs will give insights into the quark orbital angular momentum contribution to the proton spin.

Semi-inclusive deep-inelastic scattering (SIDIS) has emerged as a powerful tool to probe nucleon structure and to provide access to TMDs through measurements of spin and azimuthal asymmetries, with various experiments using semi-inclusive deep inelastic scattering (SIDIS) ($ep \to ehX$) to study TMDs which depend on the three-dimensional momentum of the parton, where a particular hadron, h, is detected in the final state.

A SIDIS reaction is one in which a beam lepton, ℓ, scatters off of a target nucleon, N, via the exchange of a photon and the scattered lepton, ℓ', is detected along with a single hadron, h; everything else in the final state, X, is ignored, i.e.,

$$\ell(k) + N(P) \to \ell'(k') + h(P_h) + X(P_X) \tag{1}$$

where k, P, k', P_h, and P_X are the 4-momenta of ℓ, N, ℓ', h, and X, respectively.

The final-state gluon radiation in SIDIS was predicted to lead to observable $\cos\phi$ modulations of the SIDIS cross section, and that effect has been proposed by Georgi and Politzer in 1977 [1] as a clean test of pQCD. Perturbative-QCD effects, like gluon radiation, can indeed lead to azimuthal dependencies in the semi-inclusive DIS cross section, but they contribute mainly at large values of P_{hT}, and are next-to-leading order in the strong coupling constant.

In 1978, Cahn [2] discussed similar asymmetries arising from non-zero intrinsic transverse momenta of partons. Although, suppressed by P_T/Q that modulation (known as the Cahn effect), appeared to be significant and dominating in the $P_{hT} \sim 1$ GeV range. Significant cosine modulations with azimuthal angle of final state hadrons with respect to the lepton scattering plane, ϕ_h, observed in various experiments indicate that higher twist effects can be very important. Additional contribution to $\cos\phi_h$ and $\cos 2\phi_h$ moments coming from processes when the final meson is produced at short distances via hard-gluon exchange [3] may also be significant in the kinematic regime where the ejected meson carries most of the virtual photon momentum.

It appeared that the interplay between the parton transverse momentum and spin (Boer-Mulders effect [4]) can generate a leading-twist contribution to the $\cos 2\phi$ modulation, which is one the main focuses of our studies.

Assuming single photon exchange, the leptoproduction cross-section for an unpolarized beam and unpolarized target can be written as a sum of structure function (see [5]) can be written as

$$\frac{d^5\sigma}{dx\ dQ^2\ dz\ d\phi_h\ dP_{h\perp}^2} = \frac{2\pi}{2(k \cdot P)x} \frac{\alpha^2}{xyQ^2} \frac{y^2}{2(1-\varepsilon)} \left(1 + \frac{\gamma^2}{2x}\right) \{F_{UU,T} \tag{2}$$

where structure functions F_{XY} depend on kinematical variables x, Q^2, z, P_{hT} define the modulations of corresponding azimuthal moments, with azimuthal angle ϕ_h, which is defined between the lepton plane and the hadron production plane according to the Trento convention [6]. The kinematic variables x, y, and z are defined as: $x = Q^2/2(P \cdot q)$, $y = (P \cdot q)/(P \cdot k)$, $z = (P_h \cdot P)/(P \cdot q)$, where $Q^2 = -q^2 = -(k - k')^2$ is the four-momentum of the virtual photon, $\gamma = 2Mx/Q$, M and M_h are the nucleon and hadron masses, P_{hT} is the transverse momentum of the detected hadron. The ratio ε of the longitudinal and transverse photon flux is given by: $\varepsilon =$

$\frac{1-y-\gamma^2 y^2/4}{1-y+y^2/2+\gamma^2 y^2/4}$. The structure function $F_{UU,T}$ defining the ϕ-integrated cross sections could be presented as a convolution of distribution function (DF), f_1, and fragmentation function (FF), D_1, which are the usual unpolarized twist-2 DF and FF, respectively.

The structure function $F_{UU}^{\cos 2\phi_h}$ at leading twist can be presented as a convolution of Boer-Mulders distribution function, $h_1^\perp$ ([4] describing the correlation between the transverse motion of a quark and its own transverse spin, and the Collins fragmentation function, $H_1^\perp$ [7], describing fragmentation of transversely polarized quarks. The structure function $F_{UU}^{\cos \phi_h}$ receives contributions from the convolution of twist-2 and twist-3 distribution and fragmentation functions, such as the twist-2 Boer-Mulders DF $h_1^\perp$ ([4, 8]), the Collins FF $H_1^\perp$, and the twist-3 DFs h and $f^\perp$ [5], which can be interpreted as a higher twist analog of the Sivers function. Both functions represent spin-orbit correlations.

The cross-section modulation of $\cos \phi$ in Eq. 2, gets contributions only at sub-leading level and suppressed by powers of the hard scale Q (higher-twist). This type of contribution is interesting in its own as it provides complementary information on the quark dynamics.

Among the various twist-3 contributions suppressed as $1/Q$, several involve either a distribution or fragmentation function that relates to quark-gluon-quark correlations, and hence is interaction dependent and has no probabilistic interpretation. In the Wandzura-Wilczeck approximation [9] all these terms are neglected, and only two contributions are considered:

$$F_{UU}^{\cos \phi} \simeq -\frac{2M}{Q} \ C \left[\frac{\hat{\mathbf{h}} \cdot \vec{p}_\perp}{M} x f^\perp D_1 + \frac{\hat{\mathbf{h}} \cdot \vec{k}_\perp}{M_h} x h H_1^\perp \right] \tag{3}$$

where the first (second) term is related to the Cahn (Boer-Mulders) effect. There are no contributions to $F_{UU}^{\cos 2\phi}$ suppressed as $1/Q$ however a contribution suppressed as $1/Q^2$ is expected from the Cahn effect to $F_{UU}^{\cos 2\phi}$. Other contributions beyond $1/Q$ have not been calculated yet. Only a few measurements of cosine modulations in semi-inclusive DIS experiments have been published in the past [10–13]. Most measurements averaged over any possible flavour dependence as they refer to hadrons without type nor charge distinction, and only to hydrogen target or hydrogen and deuterium targets combined together.

During the last few years several precise SIDIS measurements have become available. The CLAS collaboration measured non-zero cosine modulations for positive pions produced by 6 GeV/c electrons scattering off the proton [14]. The HERMES experiment have measured cosine modulations of hadrons produced in the scattering of 27.5 GeV/c electrons and positrons off pure hydrogen and deuterium targets, where the lepton beam scatters directly off neutrons and protons (with only negligible nuclear effects in case of deuterium) [15]. For the first time these modulations were determined in a four-dimensional kinematic space for positively and negatively charged pions and kaons separately, as well as for unidentified hadrons. At COMPASS, positive and negative hadrons produced by the 160 GeV/c muon beam scattering off a ^{6}LiD target have been measured in a three-dimensional grid of the relevant kinematic variables x, z and P_{hT} [16].

In all the experiments, the new data confirm the existence of a sizable $\cos \phi$ and a not-zero $\cos 2\phi$ modulations. However, the results published by different experiment appear not fully consistent. For example, positive $\cos 2\phi$ amplitudes for both positively and negatively charged hadrons were measured at COMPASS, whileat HERMES, positive $\cos 2\phi$ amplitudes were extracted for negatively charged pions, while for positively charged pions the moments are compatible with zero, but tend to be negative in some kinematic regions. In all the cases, the amplitudes of the cosine modulations show strong kinematic dependencies. The $\cos 2\phi$ modulation of positive hadrons in two experiments, while showing similar behaviour are significantly different, in particular at relatively large P_{hT} ($P_{hT} > 0.5$ GeV/c). Opposite-charge pion signals show unexpected large differences which can be related to the peculiar flavor dependence of the Collins function entering the Boer-Mulders term [15]. Disagreements are typically much bigger for integrated bins, indicating that for more complete and fair comparison between results and between results and theoretical models, a full differential analysis, using the complete multi-dimensional information is required.

The structure function $F_{UU}^{\cos \phi_h}$ is higher-twist by nature, which means it can only be accessed at moderate values of Q^2. Such higher-twist observables are a key for understanding long-range quark-gluon dynamics. They have also been interpreted in terms of average transverse forces acting on a quark at the instant after absorbing the virtual photon [17].

This letter reports measurements of structure functions for the unpolarized beam and target using SIDIS of charged pions from the e1f CLAS data set using a 5.498 GeV electron beam and the CEBAF Large Acceptance Spectrometer (CLAS) [18] at Jefferson Laboratory. Longitudinally polarized electrons were scattered off an unpolarized liquid-hydrogen target. Scattered electrons were detected in CLAS. Electron candidates were selected by a hardware trigger using a coincidence of the gas Cherenkov counters and the lead-scintillator electromagnetic calorimeters (EC).

Deep-inelastic scattering events were selected by requiring $Q^2 > 1$ GeV^2 and $W^2 > 4$ GeV^2, where W is the invariant mass of the hadronic final state. A minimum value for the $\pi^\pm$ transverse momentum, $P_T > 0.05$ GeV, ensures that the azimuthal angle ϕ_h is well-defined. The total number of selected $e\pi^\pm$ coincidences was $\approx$

$XXXXX$ for the presented z range, $0.4 < z < 0.7$, which selects the semi-inclusive region [19]. Events with missing-mass values for the $e\pi^{\pm}$ system that are smaller than 1.35 GeV ($M_x(e\pi^{\pm}) <$1.35 GeV) were discarded to exclude contributions from exclusive processes. In pion SIDIS events ($ep \rightarrow e\pi X$), the missing mass (M_X) is defined as the invariant mass of the undetected state X:

$$M_X^2 = (P + q - P_h)^2. \tag{4}$$

Figure 1 shows the M_X distribution for candidate $ep \rightarrow e\pi^{\pm}X$ events. Events with $M_X < 1.35$ GeV are cut. This cut helps to remove proton contamination at high momenta in π^+ sample, and also cuts out exclusive events ($ep \rightarrow e\pi^+n$), the peak near the nucleon mass (0.938 GeV) in figure 1) and the delta resonance (the peak near 1.2 GeV in figure 1), both of which are not desirable for a SIDIS sample anyway.
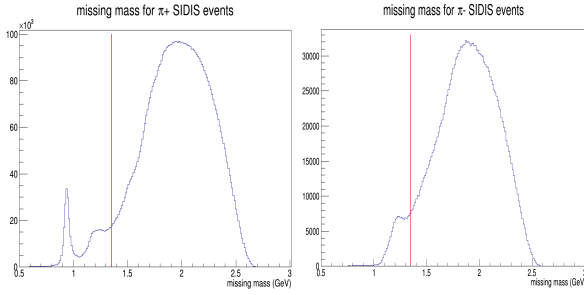

FIG. 1: The missing mass distribution for $ep \rightarrow e\pi^+X$ (left) and $ep \rightarrow e\pi^-X$ (right) events. The vertical red line shows the cut of 1.35 GeV. Events to the left of this line are removed from the sample.

A major challenge in extraction of ϕ_h distributions is the handling of the detector acceptance, both geometrical acceptance (the location of active detector elements) and the efficiency in the active regions. This is done using Monte Carlo simulations. A LUND-MC based event generator (PEPSI [?]) is used to create a realistic large set of events (several iterations may be required before the set is "realistic") which are passed through a GEANT based simulation of the CLAS detector. For a given kinematic space, the acceptance is equal to the number of reconstructed events divided by the number of generated events. The number of events in the E1-f data is then divided by the acceptance to get a corrected value for the number of events. After events have been selected and binned, and after all corrections, including bin centering corrections, have been applied, a table of values of normalized counts in elementary bin has been extracted in 5-dimensional bins in x, Q^2, z, P_T and ϕ.

HAPRAD version 2.0 [20, 21] was used to calculate radiative corrections in bins by calculating $\sigma_{rad+tail}\left(x, Q^2, z, P_{h\perp}^2, \phi_h\right)$ for a given $\sigma_{Born}\left(x, Q^2, z, P_{h\perp}^2, \phi_h\right)$ which is obtained from a model. The radiative correction factor is then simply

$$RC\,factor\left(x, Q^2, z, P_{h\perp}^2, \phi_h\right) = \frac{\sigma_{rad+tail}\left(x, Q^2, z, P_{h\perp}^2, \phi_h\right)}{\sigma_{Born}\left(x, Q^2, z, P_{h\perp}^2, \phi_h\right)} \tag{5}$$

and the Born cross-section can be obtained by dividing the measured cross-section by the RC factor, i.e., $\sigma_{Born} = \sigma_{measured}/$RC factor. Three different models were used to study model dependence of radiative corrections. The systematic error on the final result due to a given source is the RMS of the deviations of the modified result from the original, i.e. the error from source i is

$$\Delta_{RMS}^i = \frac{\sqrt{\sum_j^{N_v^i} \Delta_j^2}}{\sqrt{N_v^i}} \tag{6}$$

where Δ_j is the difference between the final result with the nominal value and the final result with variation j, and N_v^i is the number of variations for source i. Main sources of systematic uncertainties include the accetance, fitting uncertainties and structure function variations in calculations of radiative corrections. The full list is shown in Table ??

To extract multiplicities and azimuthal moments, the ϕ_h distributions for charged pions for each $x-Q^2-z-P_{h\perp}^2$ bin are fit with the function $a(1 + b\cos\phi_h + c\cos 2\phi_h)$. The parameters a, b, and c then directly give A_0, $A_{UU}^{\cos\phi_h}$, and $A_{UU}^{\cos 2\phi_h}$ for each $x - Q^2 - z - P_{h\perp}^2$ bin. A complete table of results can be found in the ancillary files. Several representitive plots are shown here in figure 2, which shows A_0, $A_{UU}^{\cos\phi_h}$, and $A_{UU}^{\cos 2\phi_h}$ vs $P_{h\perp}^2$ for several z bins for both pion channels.

A similar measurement has been published by the CLAS Collaboration using E1-6 data [14]. However, it only measures the π^+ channel and has a more limited kinematic range. A comparison for the π^+ channel in overlapping kinematic ranges is done here. In order to have a meaningful comparison, the binning scheme used here was temporarily changed to match that of [14]. Figure 3 shows the comparison between E1-f (red points) and E1-6 (black points) as a function of P_{hT}^2 for two z bins ($0.29 < z < 0.32$ (left column) and $0.32 < z < 0.35$ (right column)) for the π^+ channel. The results show clear agreement, both qualitatively and quantitatively, implying good consistency between measurements.

Different contributions to the structure function $F_{UU}^{\cos\phi_h}$ have been calculated, related to both internal quark motion and the Collins mechanisms. Sizable modulations were predicted for pion production [22] with spin-orbit correlations as the dynamical origin. Within this framework, the asymmetry generated at the distribution level is given by either the convolution of the T-odd Boer-Mulders DF $h_1^{\perp}$ with the twist-3 FF $\tilde{H}$ [5], or the convolution of the twist-3 T-odd DF $f^{\perp}$ with the unpolarized FF D_1[23]. Because the $f^{\perp}$ DF can be interpreted
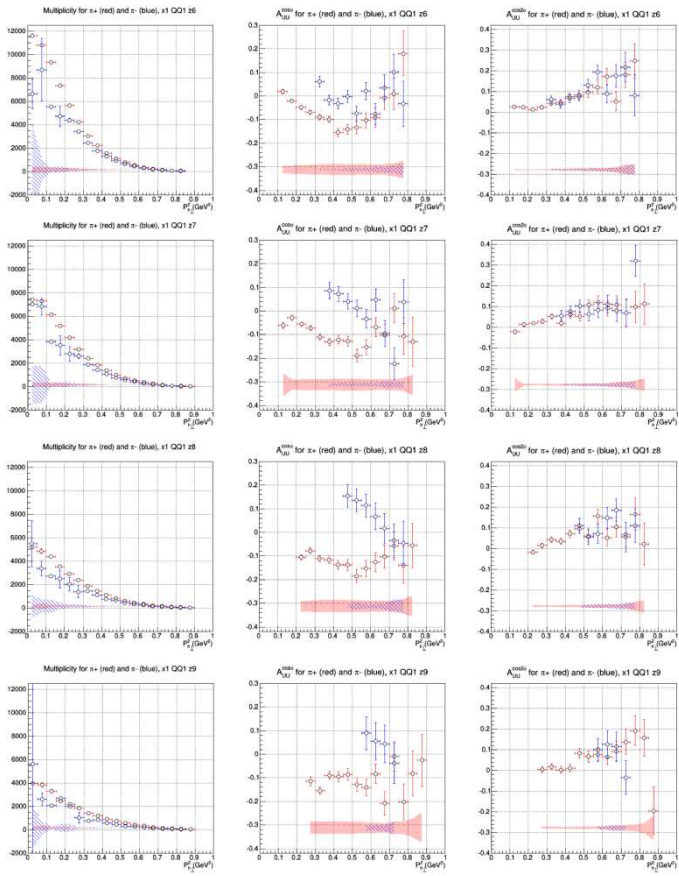
FIG. 2: A_0 (left column), $A_{UU}^{\cos\phi_h}$ (right column), and $A_{UU}^{\cos 2\phi_h}$ (right column) vs $P_{h\perp}^2$ for both pion channels. The x-Q^2 bin is fixed (the high Q^2 of $0.2 < x < 0.3$). Several z bins are shown: $0.30 < z < 0.35$ (top row), $0.35 < z < 0.40$ (second row), $0.40 < z < 0.45$ (third row), $0.45 < z < 0.50$ (bottom row).
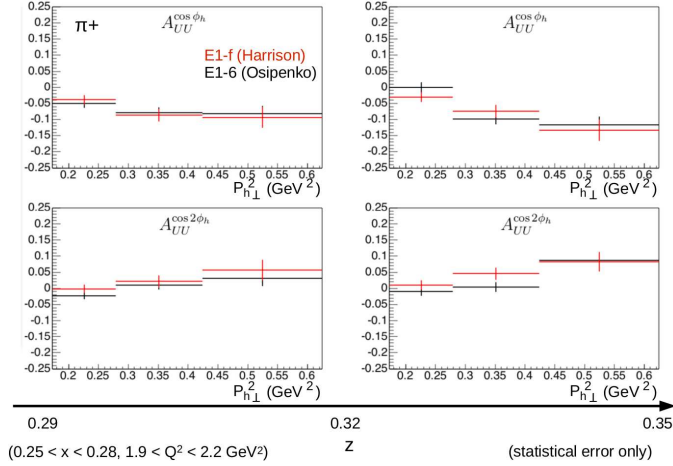

FIG. 3: $A_{UU}^{\cos\phi_h}$ (top row) and $A_{UU}^{\cos 2\phi_h}$ (bottom row) vs $P_{h\perp}^2$ for two z bins ($0.29 < z < 0.32$ (left column) and $0.32 < z < 0.35$ (right column)) for the π^+ channel for E1-f (red points) and E1-6 (black points). Only the statistical error bars are shown here.

as the higher-twist analog of the Sivers function, it underscores the potential of $\cos\phi$ modulation for studying spin-orbit correlations.

The $\cos\phi$ asymmetry gets contributions only at subleading twist and can be used to constrain the related terms [2, 3, 22]. The formalism based on the twist-3 approach could be tested in Q^2 dependence of $\cos\phi$ modulations. In the Fig. 4 CLAS measurements are compared with corresponding measurements from HERMES experiment [15]. After taking into account the kinematic factors in the expression of the $\cos\phi$ modulation and ϕ independent terms ([5])

$$f(y) \approx \frac{(2-y)\sqrt{1-y}}{1-y+y^2/2}, \tag{7}$$

The CLAS and HERMES measurements are found to be consistent with each other in a wide range of Q^2, as shown in Figs. 4, indicating that at energies as low as 5-6 GeV, the behavior of azimuthal modulations are similar to higher energy measurements. For comparison, the lowest x CLAS bin and highest x HERMES bins were used with equal average value of $x \approx 0.19$, $z \approx 0.45$ and $P_{hT} \approx 0.42$ GeV^2.

The CLAS data provide significant improvements in the precision of azimuthal moments for the kinematic region where the two data sets overlap, and they extend the measurements to the large x region not accessible at HERMES.
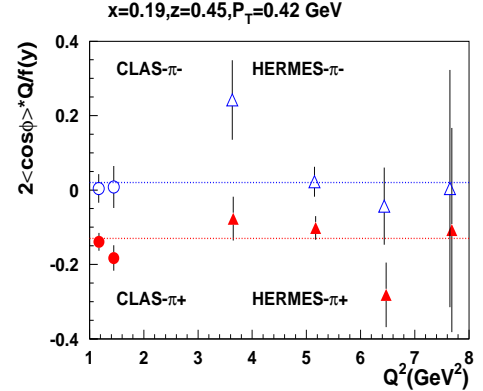

FIG. 4: (Color online) The $\cos\phi$ modulations in $\pi^{\pm}$ SIDIS plotted vs Q^2. Filled symbols are for π^+ and open symbols for π^-. The triangles CLAS and open symbols are for HERMES [15].

In summary, we have presented measurements of the kinematic dependences of the azimuthal modulations of in semi-inclusive $\pi^{\pm}$ electroproduction from the E1F CLAS data set. The $\cos\phi_h$ amplitude was extracted as a function of x and transverse pion momentum P_T, for

0.4 < z < 0.7. The moments show significant dependence on the flavor of final state. The results are compared with published HERMES data [15], providing a significant improvement in precision and can serve as an important input for studies of higher-twist effects. The Q^2-dependence of the $\cos\phi$ modulation is consistent with the twist-3 nature of the contribution and is consistent with measurements performed at much higher energies and Q^2.

[1] H. Georgi and H.D. Politzer, Phys. Rev. Lett. 40 (1978) 3.

[2] R.N. Cahn, Phys. Lett. B78 (1978) 269.

[3] E.L. Berger, Z. Phys. C4 (1980) 289.

[4] D. Boer and P.J. Mulders, Phys. Rev. D57 (1998) 5780, {\ttfamilyhep-ph/9711485}.

[5] A. Bacchetta et al., JHEP 02 (2007) 093, {\ttfamilyhep-ph/0611265}.

[6] A. Bacchetta et al., Phys. Rev. D70 (2004) 117504, {\ttfamilyhep-ph/0410050}.

[7] J.C. Collins, Nucl. Phys. B396 (1993) 161, {\ttfamilyhep-ph/9208213}.

[8] B. Pasquini and F. Yuan, Phys. Rev. D81 (2010) 114013, {\ttfamilyarXiv:1001.5398}.

[9] S. Wandzura and F. Wilczek, Phys. Lett. B72 (1977) 195.

[10] European Muon, J.J. Aubert et al., Phys. Lett. B130 (1983) 118.

[11] European Muon, M. Arneodo et al., Z. Phys. C34 (1987) 277.

[12] E665, M.R. Adams et al., Phys. Rev. D48 (1993) 5057.

[13] ZEUS, J. Breitweg et al., Phys. Lett. B481 (2000) 199, {\ttfamilyhep-ex/0003017}.

[14] CLAS, M. Osipenko et al., Phys. Rev. D80 (2009) 032004, {\ttfamilyarXiv:hep-ex/0809.1153}.

[15] HERMES Collaboration, A. Airapetian et al., Phys.Rev. D87 (2013) 012010, {\ttfamilyarXiv:1204.4161}.

[16] COMPASS, C. Adolph et al., Nucl. Phys. B886 (2014) 1046, {\ttfamilyarXiv:1401.6284}.

[17] M. Burkardt, hep-ph 0807.2599 (2008), {\ttfamilyarXiv:hep-ph/0807.2599}.

[18] CLAS Collaboration, B. Mecking et al., Nucl.Instrum.Meth. A503 (2003) 513.

[19] CLAS Collaboration, H. Avakian et al., Phys. Rev. Lett. 105 (2010) 262002, {\ttfamilyarXiv:hep-ex/1003.4549}.

[20] I. Akushevich, N. Shumeiko and A. Soroko, Eur. Phys. J. C10 (1999) 681, {\ttfamilyhep-ph/9903325}.

[21] I. Akushevich, A. Ilyichev and M. Osipenko, Phys.Lett. B672 (2009) 35, {\ttfamilyarXiv:0711.4789}.

[22] M. Anselmino et al., Phys. Rev. D71 (2005) 074006, {\ttfamilyhep-ph/0501196}.

[23] A. Metz and M. Schlegel, Eur. Phys. J. A22 (2004) 489, {\ttfamilyhep-ph/0403182}.

$< P_T >$	$< z >$	$< x >$	$< Q^2 >$	$< y >$	A0	$A_{UU}^{\cos\phi_h}$	$A_{LU}^{\cos 2\phi_h}$	$\pm stat.$	$\pm syst.$
0.138	0.507	0.160	1.36	0.786	0.786	0.786	0.0081	0.0054	0.0053
0.138	0.507	0.160	1.36	0.786	0.786	0.786	0.0081	0.0054	0.0053

TABLE I: The multiplicity (A_0) and moments $A_{UU}^{\cos\phi_h}$ and $A_{UU}^{\cos 2\phi_h}$ and their statistical and systematic uncertainties at average values of P_T, z, x, Q^2 and y. An additional 3% uncertainty from relative uncertainty from radiative effects should be added to the total uncertainty.

$< P_T >$	$< z >$	$< x >$	$< Q^2 >$	$< y >$	A0	$A_{UU}^{\cos\phi_h}$	$A_{LU}^{\cos 2\phi_h}$	$\pm stat.$	$\pm syst.$
0.138	0.507	0.160	1.36	0.786	0.786	0.786	0.0081	0.0054	0.0053
0.138	0.507	0.160	1.36	0.786	0.786	0.786	0.0081	0.0054	0.0053